



Structure of the prompt neutron multiplicity distribution in the spontaneous fission of ^{256}Rf

A.V. Isaev^{a,*}, R.S. Mukhin^a, A.V. Andreev^a, Z. Asfari^b, M.L. Chelnokov^a, V.I. Chepigin^a, H.M. Devaraja^a, O. Dorvaux^b, B. Gall^b, K. Hauschild^c, I.N. Izosimov^a, A.A. Kuznetsova^a, A. Lopez-Martens^c, O.N. Malyshev^{a,d}, A.G. Popeko^{a,d}, Yu.A. Popov^{a,d}, A. Rahmatinejad^a, B. Sailaubekov^{a,e,f}, T.M. Shneidman^{a,g}, E.A. Sokol^a, A.I. Svirikhin^{a,d}, M.S. Tezekbayeva^{a,e}, A.V. Yeremin^{a,d}, N.I. Zamyatin^a

^a Joint Institute for Nuclear Research, Dubna, 141980, Russia

^b Université de Strasbourg, CNRS, IPHC, Strasbourg, UMR7178, 67037, France

^c IJCLab, IN2P3-CNRS, Université Paris-Saclay, Orsay, UMR9012, 91405, France

^d Dubna State University, Dubna, 141980, Russia

^e Institute of Nuclear Physics, Almaty, 050032, Kazakhstan

^f L.N. Gumilyov Eurasian National University, Astana, 010000, Kazakhstan

^g Kazan Federal University, Kazan, 420008, Russia

ARTICLE INFO

Article history:

Received 14 December 2022

Received in revised form 16 May 2023

Accepted 6 June 2023

Available online 12 June 2023

Editor: B. Blank

Keywords:

Superheavy nuclei
Spontaneous fission
Prompt neutrons
Fission modes

ABSTRACT

An experimental study of ^{256}Rf spontaneous fission following the fusion reaction of $^{50}\text{Ti}+^{208}\text{Pb}$ was performed using the velocity filter SHELS of the Flerov laboratory at JINR. The average number of neutrons of $\bar{\nu} = 4.30 \pm 0.17$ and variance of $\sigma_{\nu}^2 = 3.2$ from the prompt neutron multiplicity distribution were obtained. The alpha decay branching ratio of $b_{\alpha} = 0.003^{+0.005}_{-0.003}$ and the half-life of $T_{1/2} = (6.7 \pm 0.2)$ ms of the isotope were determined. For the first time, our neutron detector system allowed us to extend investigation of the prompt neutron multiplicity study to the superheavy element region.

© 2023 The Author(s). Published by Elsevier B.V. This is an open access article under the CC BY license (<http://creativecommons.org/licenses/by/4.0/>). Funded by SCOAP³.

1. Introduction

This paper discusses the search for fission modes using shapes of prompt neutron multiplicity distributions. For the ^{256}Rf nucleus, bimodal fission can manifest itself in both TKE spectra and the prompt neutron multiplicity distribution. It will be shown that, the prompt neutron multiplicity distributions can have a structure and therefore carry valuable information about the mechanism of nuclear fission.

The spontaneous fission process was discovered for uranium in 1940 by G.N. Flerov and K.A. Petrzhak [1]. The energy of the fission reaction is predominantly released as the kinetic energy of the fission fragments. However, a significant part of the energy is also spent on the excitation of fragment nuclei, which can then de-excite by evaporating prompt neutrons. The shell structure and

deformations of the forming fragments affect the excitation energy, which is reflected in the dependence of the average number of prompt neutrons on the mass number of the fission fragment. This dependence has a “sawtooth” shape with minima, related to magic nuclei [2].

The neutron multiplicity distributions can be used to improve theoretical approaches to nuclear fission. Obtaining data on neutron yields is especially important and at the same time challenging for short-lived heavy nuclei in the region $Z \geq 100$. Because of the low production rates of transfermium nuclei, high overall neutron detection efficiency is an essential requirement for any detector system used in online experiments. In this context, the development of an efficient neutron detector at the Flerov Laboratory of Nuclear Reactions (FLNR) [3] has made it possible to study the spontaneous fission neutron multiplicities in the transfermium and superheavy regions. Studies down to the nanobarn production cross-section level are achieved.

In the present work, for the first time, a detailed experimental study of the neutron multiplicity distribution in the spontaneous

* Corresponding author.

E-mail address: isaev@jinr.ru (A.V. Isaev).

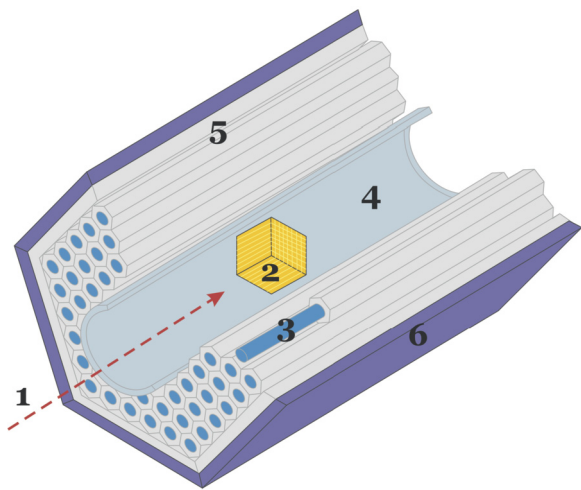


Fig. 1. Cutaway view of the detection system installed at SHELs to investigate neutron multiplicity: 1 – recoil nuclei; 2 – Si-detector array; 3 – ^3He -counters; 4 – vacuum chamber; 5 – moderator; 6 – borated polyethylene shield.

fission of superheavy nuclei ^{256}Rf is presented. The results are discussed with previously measured nuclei ^{260}Md and ^{252}No together with the calculations of GEF (“General description of Fission observables”) [4] and ISP (“Improved Scission-Point”) [5,6] models.

2. Experimental details

The experiment was carried out at the FLNR JINR. The velocity filter SHELs [7] was used to separate the ^{256}Rf recoils from all other reaction products and primary beam. The selected ^{256}Rf recoils pass through the SHELs separator and time of flight (TOF) detectors and, finally, are implanted into the detection system. The detector system includes 54 ^3He -neutron counters [3] placed around an assembly (“well” like) of Si detectors [8]. The Si detectors array consists of a 48×48 -strip focal-plane detector and 4 tunnel 16-strip detectors for fission-fragment and α -particle registration. The neutron counters allow the detection of multiple prompt neutrons emitted in the spontaneous fission process of the nucleus (Fig. 1).

The high granularity of the neutron detector enabled us to register multiple neutron events at a time. Consequently, the probability of detecting several neutrons simultaneously in a single ^3He -counter within the coincidence time window is negligible. The neutron registration efficiency, measured with a ^{248}Cm source is $(45 \pm 1)\%$, and the average neutron lifetime in the assembly is $(23 \pm 1) \mu\text{s}$. The detection efficiency of the focal-plane Si detector for α -particles emitted by implanted nuclei is $\sim 50\%$ and 100% for the detection of at least one of the two fission fragments. Once a fission fragment is detected in the focal-plane DSSD, the signal from the fast output of the spectrometry amplifier triggers the neutron counter circuit interrogation for a duration of 128 μs with a 1 μs time step.

The complete fusion reaction $^{208}\text{Pb}(^{50}\text{Ti}, 2n)^{256}\text{Rf}$ was used to synthesize the investigated rutherfordium isotope. The ^{50}Ti ions were accelerated by the U-400 cyclotron up to an energy of $(237 \pm 3) \text{ MeV}$. The PbS target thickness was $350 \mu\text{g}/\text{cm}^2$ (the ^{208}Pb isotope enrichment $> 99\%$), and a 2 μm thick titanium backing was used. The total number of beam ions that passed through the target and then stopped in a faraday cup was about 2.8×10^{18} .

3. Results

Fission fragments from ^{256}Rf spontaneous fission were searched for the time interval $(0 - 62) \text{ ms}$ ($\sim 10 \times T_{1/2}$) following the registration of the implanted reaction products. A total number of

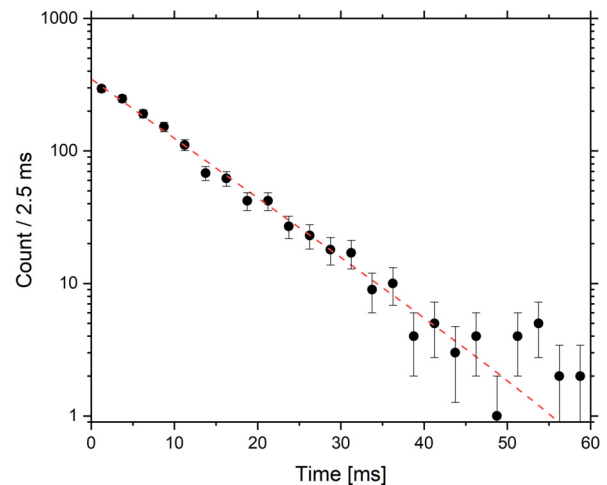


Fig. 2. Distribution of time differences between recoil nuclei and fission-fragment registration for ^{256}Rf : the symbols represent the experimental data and the dashed line is the fit using the exponential decay function.

Table 1

Prompt neutron measured (F_n) and emitted (P_n) probabilities for ^{256}Rf spontaneous fission. Where n is the neutron multiplicity, ΔF_n and ΔP_n are the corresponding uncertainties, \sum_{SF} is number of spontaneous fission events observed in the experiment for the given n .

n	\sum_{SF}	F_n	ΔF_n	P_n	ΔP_n
0	199	0.148	0.010	0.042	0.014
1	348	0.259	0.014	0.062	0.018
2	343	0.255	0.010	0.062	0.021
3	290	0.215	0.007	0.102	0.021
4	129	0.096	0.004	0.192	0.022
5	32	0.024	0.002	0.253	0.022
6	3	0.002	0.001	0.205	0.019
7	1	0.001	< 0.001	0.082	0.018
8	0	0	< 0.001	0	0.014

1345 ^{256}Rf spontaneous fissions were found during the data analysis. The ^{256}Rf half-life was obtained as $T_{1/2} = (6.7 \pm 0.2) \text{ ms}$ from the time distribution shown in Fig. 2. The value is in good agreement with the previously-measured values of $(6.2 \pm 0.2) \text{ ms}$ [9], $(6.7 \pm 0.2) \text{ ms}$ [10], $(6.9 \pm 0.4) \text{ ms}$ [11] and $(6.9 \pm 0.2) \text{ ms}$ [12].

To determine the alpha decay branching ratio, “Recoil – α_1 – α_2 ” correlations were used. The α_1 was searched for within a time interval $(0 - 62) \text{ ms}$ from the recoil implantation signal, whereas the α_2 was searched for in the time interval of $(0 - 23) \text{ s}$ from α_1 . Only one correlation was found, where all the α decay events localized in the same pixel of the focal plane detector (^{256}Rf : 6.015 ms and 8714 keV; ^{252}No : 2.69 s and 8373 keV). By considering the 25% registration efficiency for our one α decay chain event in the focal-plane detector, the α decay branching ratio is $b_\alpha = 0.003^{+0.005}_{-0.003}$. The obtained b_α agrees with the previously published value of 0.0032 ± 0.0017 [9].

Prompt neutrons emitted in the spontaneous fission of ^{256}Rf were searched for in the time interval $(0 - 128) \mu\text{s}$ from the moment of the fission-fragment registration in the focal-plane DSSD. A total number of 2605 prompt neutrons in correlation with 1345 ^{256}Rf spontaneous fission events were registered. The neutron yield data (Table 1) were obtained for the first time. After taking into account the detector efficiency $(45 \pm 1)\%$, the emitted neutron distribution properties were obtained: the mean as $\bar{\nu} = 4.30 \pm 0.17$ and the variance as $\sigma_\nu^2 = 3.2$.

The Tikhonov statistical regularization method [13–15] was applied to extract the emission probabilities P_n from the measured ones F_n . The reconstruction results are shown in Fig. 3 and Table 1.

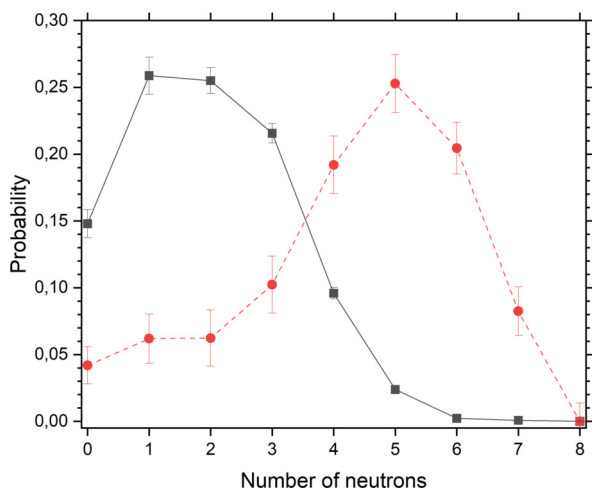


Fig. 3. Probability distributions for the neutrons from the spontaneous fission of ^{256}Rf : measured in the experiment F_n (squares) and reconstructed P_n (circles). The lines have been added to guide the eye.

For the reconstructed distribution, the average number of neutrons is 4.33 ± 0.14 and the variance is 3.3.

An important task in the experiment was to provide protection against neutrons and γ -quanta produced in the target and in the Faraday cup of the SHELS separator. The dipole magnet located upstream of the detecting system deflected the evaporation residues by 8° and thus removed the detector's illumination along the separator axis [7]. The detecting system was located behind a wall of heavy concrete about 2 meters thick. Additional protection of the detector from the background was provided by a shield made of 5%-borated polyethylene of 5 cm thickness [3]. During the operation of the U-400 cyclotron, the background neutron counting rate was about 100 neutrons/s inside the detector. Neutron signals were separated from γ -quanta signals by setting the thresholds of discriminators. The influence of the background on the shape of the prompt neutron multiplicity distribution was insignificant in comparison with the level of statistical uncertainties obtained in the experiment. The background-to-signal ratio is about 1% whereas the relative statistical uncertainty is about 4%.

4. Discussion

The theoretical calculations of neutron multiplicity were carried out in the frame of the ISP model. The details of the model are presented in [5,6]. In short, the model assumes that after crossing the fission barrier, a fissile nucleus can be described as a superposition of binary systems, specified by the masses, charges, and deformations of its constituent fragments. The potential energy surface is calculated in the mic-mac approach with an account for the shell corrections of the fragments and their damping with excitation energy. The weights of binary systems are determined by their level densities.

The model showed good results for the description of fission observables in the actinide region [16]. In [17], it was realized that to deal with the spontaneous fission of heavier nuclei, the ISP model has to be modified to account for the evolution of the fissile nucleus towards the scission point. It was done by incorporating the additional deformation cut-off function, which ensures that binary systems decay before reaching the configurations with large deformations of the fragments [17].

An attempt to use the same approach for ^{256}Rf showed that the parameters of the cut-off function can not be taken in a universal way. Therefore, here we explicitly treated the evolution of the initial distribution of the binary systems solving a master equation

for a random walk on the potential energy surface calculated in the ISP model. Previously, an analogous approach was applied for the description of observables in deep inelastic reactions [18]. The model describing fission as the Brownian shape motion on a potential energy surface in five-dimensional deformation space was developed in [19].

The transition probabilities for change of the deformations, masses, and charges of the fragments were evaluated simultaneously with the probability to overcome a barrier in the interaction potential between the fragments of the binary system (thus undergoing fission). The transition probabilities were taken proportional to the level density of the corresponding final states $\rho_f(U_f^*)$ to ensure the detailed balance principle between the direct and reverse transitions: $P_{i \rightarrow f}/P_{f \rightarrow i} = \rho_i(U_i^*)/\rho_f(U_f^*)$. The level densities $\rho(U^*)$ are taken in the form of a Fermi gas distribution with the level density parameters depending on the mass number as $a = A/12$. For the decay probability, the level density is taken at the top of the barrier in the interaction potential.

To determine the initial distribution of the binary systems, we fixed the quadrupole moment Q_{20} of the fissile nucleus to fulfill that, first, the nucleus has already crossed the fission barrier and, second, that there are a significant amount of binary systems with quadrupole moments in the 10% range around Q_{20} . The value Q_{20} was fixed to give the best description of the average neutron number in spontaneous fission of ^{260}Md , ^{256}Rf and ^{252}No nuclei which yields the value of Q_{20} corresponding to the quadrupole deformation parameter of the fissile nucleus $\beta_{20} = 1.15$.

The details of the calculations and the application of the model to various nuclei will be presented in a forthcoming publication [20].

The theoretical calculations were performed for ^{260}Md , ^{256}Rf and ^{252}No . For a small number of evaporated neutrons, the behaviour of the neutron multiplicity distribution for ^{260}Md and ^{256}Rf is similar. At the same time, ^{252}No is given to show that the behaviour at low neutron multiplicities can differ significantly for other nuclei. For a comparative analysis, the calculations were also carried out with GEF model [4]. In Fig. 4, the calculation results along with our experimental results are presented. The ISP model predicts the average numbers of neutrons in the spontaneous fission processes, which agree with the values measured in experiments for ^{256}Rf and ^{252}No nuclei (see Table 2). The GEF model underestimates the $\bar{\nu}$ values for ^{260}Md and ^{256}Rf . Regarding the shape of the prompt neutron multiplicity distributions, the ISP model provides a better prediction for ^{256}Rf , while the GEF model predicted well for ^{252}No .

The experiment shows a significant number ($\sim 10\%$) of ^{256}Rf spontaneous fission events accompanied by the emission of at most one prompt neutron. A similar and more pronounced effect was observed previously [21] for ^{260}Md (Fig. 4), where bimodal symmetric fission was discovered [23]. This behaviour of the neutron multiplicity distributions of ^{256}Rf and ^{260}Md is strikingly different from what we see for ^{252}No (see Fig. 4).

As shown in [24], the experimental TKE distribution of ^{256}Rf contains two components. Two fission modes of ^{256}Rf also were predicted by theoretical calculations [25], that showed that a high-energy TKE component characterized by a symmetric mass distribution of fission fragments, while a low-energy TKE component corresponds to an asymmetric mass distribution of fission fragments.

The calculations of TKE distribution and mass distribution of fission fragments were performed in the ISP model. The results of the calculations are shown in Fig. 5 for various groups of multiplicities of emitted prompt neutrons, as well as for cumulative total contributions. The rise in the left tail of the neutron multiplicity distribution can be explained by the presence of spontaneous fission events for which the reaction energy is mainly released in the

Table 2
Comparison of experimental and theoretical prompt neutron multiplicity distributions for ^{260}Md , ^{256}Rf and ^{252}No .

Isotope	Property	Experiment			Model	
		[21]	This work	[22]	ISP	GEF
^{260}Md	$\bar{\nu}$	2.58 ± 0.11	–	–	2.25	1.86 ± 0.04
	σ_ν^2	2.6	–	–	3.4	1.0
^{256}Rf	$\bar{\nu}$	–	4.30 ± 0.17	–	4.30	2.83 ± 0.12
	σ_ν^2	–	3.2	–	2.5	2.6
^{252}No	$\bar{\nu}$	–	–	4.25 ± 0.09	4.22	4.04 ± 0.01
	σ_ν^2	–	–	2.1	1.4	1.6

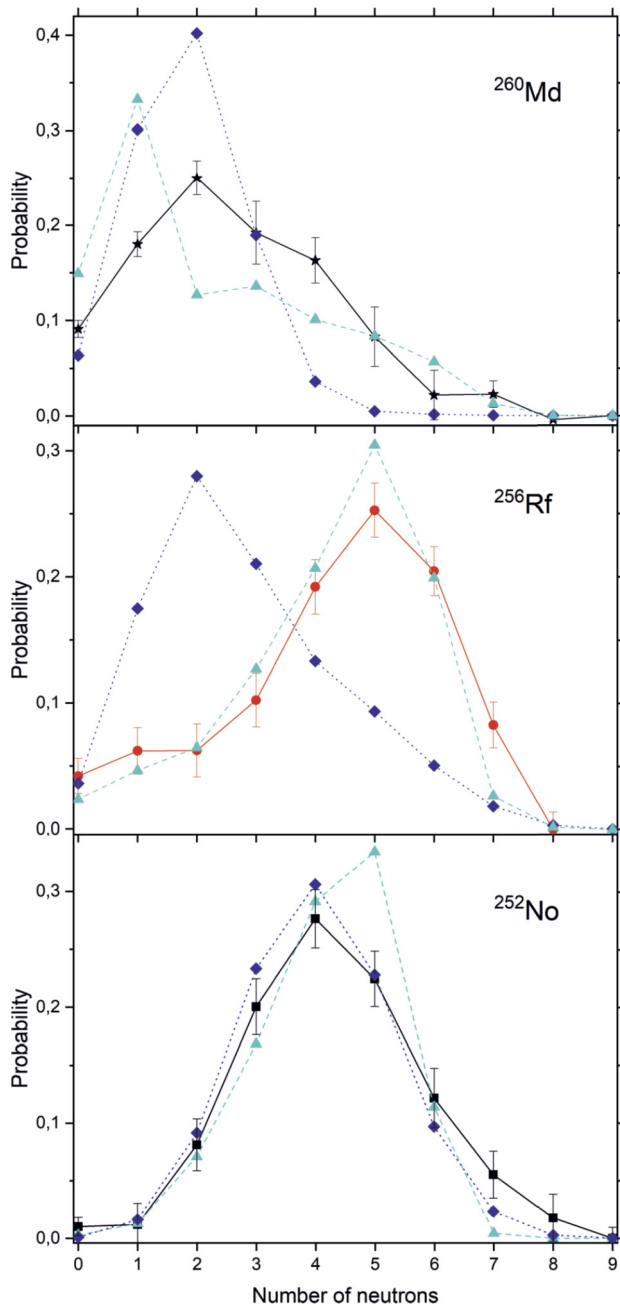


Fig. 4. Prompt neutron emission probability distributions for ^{260}Md (top), ^{256}Rf (center) and ^{252}No (bottom). Theoretical calculations: triangles – ISP model; rhombuses – GEF model [4]. Experimental data: stars – data from [21]; circles – values obtained in this work; squares – data from [22]. The lines connecting points have been added for clarity.

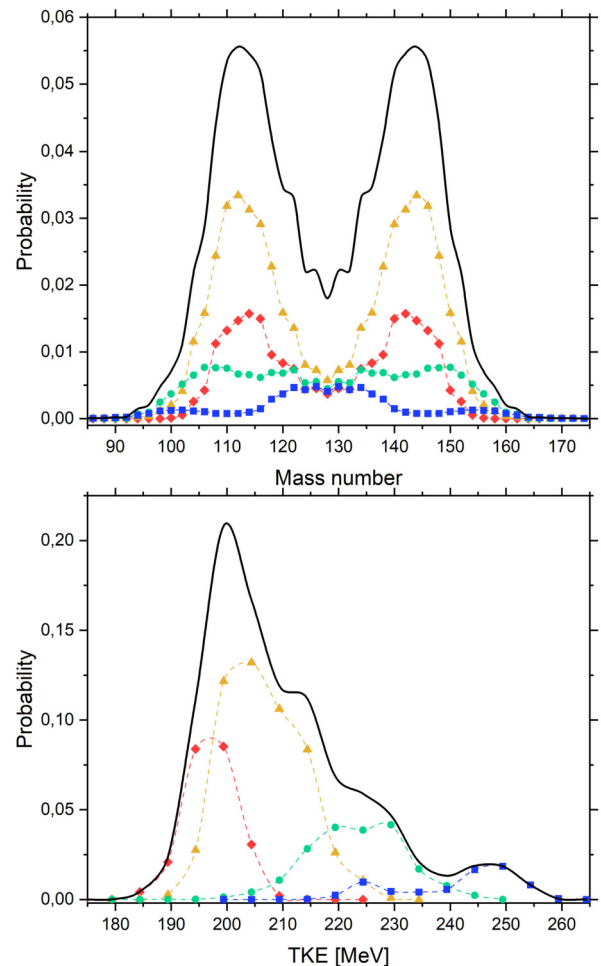


Fig. 5. Calculated mass distributions of fission fragments (top) and TKE distributions (bottom) for ^{256}Rf spontaneous fission. Results grouped by multiplicities of emitted prompt neutrons (n): solid line – overall by all multiplicities; squares – from $0n$ to $1n$; circles – from $2n$ to $3n$; triangles – from $4n$ to $5n$ and rhombuses – from $6n$ to $9n$.

form of the kinetic energy of fission fragments (Fig. 5). Thus the effect is may be related to the contribution of the symmetric fission mode of ^{256}Rf .

5. Conclusions

The prompt-neutron emission probabilities of different multiplicities were observed in the spontaneous fission of ^{256}Rf . The average number of neutrons in the spontaneous fission process was found to be $\bar{\nu} = 4.30 \pm 0.17$ while the variance is $\sigma_\nu^2 = 3.2$.

Structure is revealed in prompt neutron multiplicity distribution of ^{256}Rf . The experimentally observed increased probability for low

neutron multiplicities is most likely associated with the compact fission mode of ^{256}Rf . This mode is characterized by large values of the average total kinetic energy and (as a consequence) by lower neutron evaporation. The ability to see the structure in the distributions of prompt neutrons is extremely important for determining fission modes. Especially it concerns spontaneously fissile nuclei where there is no data on the total kinetic energy and mass distributions of fission fragments.

The experimental results for ^{256}Rf are compared with predictions made by the ISP model. The agreement found in the average number of neutrons in the spontaneous fission processes is good and the shape of the model distribution is quite close to the experimental one.

Funding

This work was supported by the Russian Foundation for Basic Research (project no. 18-52-15004), and the Joint Institute for Nuclear Research (grant no. 22-502-06). T.M.S. was partly supported by the Kazan Federal University Strategic Academic Leadership Program.

Declaration of competing interest

The authors declare that they have no known competing financial interests or personal relationships that could have appeared to influence the work reported in this paper.

Data availability

Data will be made available on request.

References

- [1] G.N. Flerov, K.A. Petrjak, Spontaneous fission of uranium, *Phys. Rev.* 58 (1940) 89, <https://doi.org/10.1103/PhysRev.58.89.2>.
- [2] J. Gindler, Dependence of neutron yield on fragment mass for several low-energy fissioning systems, *Phys. Rev. C* 19 (1979) 1806–1819, <https://doi.org/10.1103/PhysRevC.19.1806>.
- [3] A.I. Svirikhin, et al., A detector for studying the characteristics of spontaneous fission of short-lived heavy nuclei, *Instrum. Exp. Tech.* 54 (5) (2011) 644–648, <https://doi.org/10.1134/S0020441211040154>.
- [4] K.-H. Schmidt, et al., General description of fission observables: GEF model code, *Nucl. Data Sheets* 131 (2016) 107–221, <https://doi.org/10.1016/j.nds.2015.12.009>.
- [5] A.V. Andreev, et al., Possible explanation of fine structures in mass-energy distribution of fission fragments, *Eur. Phys. J. A* 22 (1) (2004) 51–60, <https://doi.org/10.1140/epja/i2004-10017-9>.
- [6] A.V. Andreev, et al., Ternary fission within statistical approach, *Eur. Phys. J. A* 30 (3) (2006) 579–589, <https://doi.org/10.1140/epja/i2006-10145-2>.
- [7] A.G. Popeko, et al., Separator for heavy Element spectroscopy – velocity filter SHELS, *NIM B* 376 (2016) 140–143, <https://doi.org/10.1016/j.nimb.2016.03.045>.
- [8] A.V. Isaev, et al., Application of a double-sided stripped Si detector in the focal plane of the VASILISSA separator, *Instrum. Exp. Tech.* 54 (1) (2011) 37–42, <https://doi.org/10.1134/S00204412110061028>.
- [9] F.P. Heßberger, et al., Spontaneous fission and alpha-decay properties of neutron deficient isotopes 104 and $^{258}106$, *Z. Phys. A, Hadrons Nucl.* 359 (4) (1997) 415–425, <https://doi.org/10.1007/s002180050422>.
- [10] Yu.Ts. Oganessian, et al., On the stability of the nuclei of element 108 with $A = 263$ –265, *Z. Phys. A, Hadrons Nucl.* 319 (1984) 215–217, <https://doi.org/10.1007/BF01415635>.
- [11] A.P. Robinson, et al., Search for a 2-quasiparticle high-K isomer in ^{256}Rf , *Phys. Rev. C* 83 (2011) 064311, <https://doi.org/10.1103/PhysRevC.83.064311>.
- [12] P.T. Greenlees, et al., Shell-structure and pairing interaction in superheavy nuclei: rotational properties of the nucleus ^{256}Rf , *Phys. Rev. Lett.* 109 (2012) 012501, <https://doi.org/10.1103/PhysRevLett.109.012501>.
- [13] V.F. Turchin, V.P. Kozlov, M.S. Malkevich, The use of mathematical-statistics methods in the solution of incorrectly posed problems, *Sov. Phys. Usp.* 13 (6) (1971) 681–703, <https://doi.org/10.1070/psu1971v013n06abeh004273>.
- [14] V.F. Turchin, Solution of the Fredholm equation of the first kind in a statistical ensemble of smooth functions, *USSR Comput. Math. Math. Phys.* 7 (6) (1967) 79–96, [https://doi.org/10.1016/0041-5553\(67\)90117-6](https://doi.org/10.1016/0041-5553(67)90117-6).
- [15] R.S. Mukhin, et al., Reconstruction of spontaneous fission neutron multiplicity distribution spectra by the statistical regularization method, *PEPAN Lett.* 18 (4) (2021) 439–444, <https://doi.org/10.1134/S1547477121040130>.
- [16] H. Paşca, et al., Simultaneous description of charge, mass, total kinetic energy, and neutron multiplicity distributions in fission of Th and U isotopes, *Phys. Rev. C* 104 (2021) 014604, <https://doi.org/10.1103/PhysRevC.104.014604>.
- [17] A.V. Isaev, et al., Prompt neutron emission in the spontaneous fission of ^{246}Fm , *Eur. Phys. J. A* 58 (6) (2022) 108, <https://doi.org/10.1140/epja/s10050-022-00761-3>.
- [18] G.G. Adamyan, et al., Influence of shell effects on the dynamics of deep inelastic heavy-ion collisions, *Phys. Part. Nucl.* 25 (6) (1994) 583–611.
- [19] J. Randrup, P. Möller, Brownian shape motion on five-dimensional potential-energy surfaces: nuclear fission-fragment mass distributions, *Phys. Rev. Lett.* 106 (2011) 132503, <https://doi.org/10.1103/PhysRevLett.106.132503>.
- [20] A.V. Andreev, et al., EPJ, in preparation.
- [21] J.F. Wild, et al., Prompt neutron emission from the spontaneous fission of ^{260}Md , *Phys. Rev. C* 41 (1990) 640–646, <https://doi.org/10.1103/PhysRevC.41.640>.
- [22] A.V. Isaev, et al., The SFiNx detector system, *PEPAN Letters* 19 (1) (2022) 37–45, <https://doi.org/10.1134/S154747712201006X>.
- [23] E.K. Hulet, et al., Spontaneous fission properties of ^{258}Fm , ^{259}Md , ^{260}Md , ^{258}No , and $^{260}104$: Bimodal fission, *Phys. Rev. C* 40 (1989) 770–784, <https://doi.org/10.1103/PhysRevC.40.770>.
- [24] P. Mosat, et al., K isomerism in ^{255}Rf and total kinetic energy measurements for spontaneous fission of $^{255,256,258}\text{Rf}$, *Phys. Rev. C* 101 (2020) 034310, <https://doi.org/10.1103/PhysRevC.101.034310>.
- [25] N. Carjan, et al., Fission of transactinide elements described in terms of generalized Cassinian ovals: fragment mass and total kinetic energy distributions, *Nucl. Phys. A* 942 (2015) 97–109, <https://doi.org/10.1016/j.nuclphysa.2015.07.019>.